

---

# OPENCFS-DATA: DATA PRE-POST-PROCESSING TOOL FOR OPENCFS - AEROACOUSTICS SOURCE FILTERS

---

A PREPRINT

**Stefan Schoder**

Group of Aeroacoustics and Vibroacoustics, IGTE  
TU Graz  
Inffeldgasse 18, 8010 Graz  
stefan.schoder@tugraz.at

**Klaus Roppert**

Group of Multiphysics, IGTE  
TU Graz  
Inffeldgasse 18, 8010 Graz  
klaus.roppert@tugraz.at

February 8, 2023

## ABSTRACT

Many numerical simulation tools have been developed and are on the market, but there is still a strong need for appropriate tools capable to simulate multi-field problems, especially in aeroacoustics. Therefore, openCFS provides an open-source framework for implementing partial differential equations using the finite element method. Since 2000, the software has been developed continuously. The result of is openCFS (before 2020 known as CFS++ Coupled Field Simulations written in C++). In this paper, we present for the first time the CFS-Data, the open-source pre-post-processing part of openCFS with a focus on the aeroacoustic source computation (called filters).

**Keywords** Open Source FEM Software · Multiphysics Simulation · C++ · Acoustics · Aero-Acoustics · openCFS

## 1 Introduction

Within this contribution, we concentrate on the openCFS [31] module *openCFS-Data*. Several publications presented details on the module [38, 23, 39], and applied it to special aeroacoustic source models [7, 34, 21, 23, 44, 22, 25, 11], and special wave equation models [8, 17] are available. Since 2016, the software provided solutions for challenges in acoustical engineering and medicine. Car frame noise [1, 3, 27, 44, 16], fan noise [20, 40, 6, 10, 37, 41, 42, 19, 35] noise emissions of the turbocharger compressor [5, 9, 4], HVAC systems were computed. For post-processing, the fluid field was decomposed into a longitudinal and transversal processes [33, 32, 24, 29]. Furthermore, the human phonation process is studied in detail [36, 43, 45, 28, 2, 13, 15, 30, 14, 26, 18, 12].

When establishing an XML file for CFS-Data, it is fundamental that the pipeline, existing of different CFS-Data filters, is closed. The pipeline has to start with the step value definition and has to be followed by the input filter and end with the output filter. In between, multiple filters can be added, serial or parallel.

**Defining Step Value Definition:** It is possible to define input data for the time and frequency domain. However, not all filters are capable of processing data in the frequency domain.

```
<pipeline>
  <stepValueDefinition>
    <startStop>
      <startStep value="..."/>
      <numSteps value="..."/>
      <startTime value="..."/>
      <delta value="..."/>
      <deleteOffset value="no"/>
    </startStop>
  </stepValueDefinition>
```

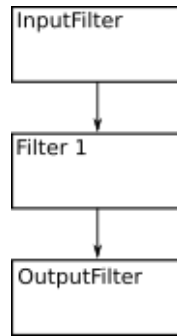


Figure 1: Serial alignment of a filter.

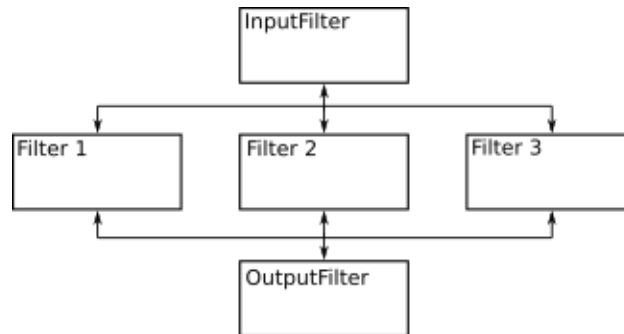


Figure 2: Parallel alignment of filters in a pipeline.

```
</pipeline>
```

Filters can be designed and aligned in a serial or parallel way (see Fig. 1 and 2).

Such a serial alignment results in the following structure.

```
<pipeline>
  <stepValueDefinition>
    <startStop>
      <startStep value="..." />
      <numSteps value="..." />
      <startTime value="..." />
      <delta value="..." />
      <deleteOffset value="no" />
    </startStop>
  </stepValueDefinition>

  <meshInput id="inputFilter" gridType="fullGrid" >

</meshInput>

  <interpolation type="FieldInterpolation_Cell2Node" id="interp1" inputFilterIds="inputFilter">
</interpolation>

  <meshOutput id="Outout" inputFilterIds="interp1">

</meshOutput>
</pipeline>
```

whereas a parallel alignment is set up in the following.

```
<pipeline>
```

```

<stepValueDefinition>
  <startStop>
    <startStep value="..."/>
    <numSteps value="..."/>
    <startTime value="..."/>
    <delta value="..."/>
    <deleteOffset value="no"/>
  </startStop>
</stepValueDefinition>

<meshInput id="inputFilter" gridType="fullGrid" >

</meshInput>

<interpolation type="FieldInterpolation_Cell2Node" id="interp1" inputFilterIds="inputFilter">
</interpolation>

<interpolation type="FieldInterpolation_Cell2Node" id="interp2" inputFilterIds="inputFilter">
</interpolation>

<interpolation type="FieldInterpolation_Cell2Node" id="interp3" inputFilterIds="inputFilter">
</interpolation>

<meshOutput id="Outout" inputFilterIds="interp1 interp2 interp3">

</meshOutput>
</pipeline>

```

Within the pipeline, different filters can be arranged. The following filter classes are available today:

- Interpolation Filters
- Conservative Interpolation Filters
- Aeroacoustic Source Terms
- Synthetic Sources
- Data Processing

In this contribution, we discuss the input format, output format and Aeroacoustic Source Terms (filter) in more detail.

## 2 IO Formats and Definitions

The data processing tool of openCFS offers the option of importing Enight-files and hdf5-files (hierarchical data format), whereas the export of mesh-based field data is by default based on hdf5, which is the native data format of openCFS. Additionally, reading of meshes (e.g. target mesh for interpolation) in cgns or cdb format is supported. Field data can thereby be defined on the nodes or the cell centroids of a computational grid in the time or the frequency domain.

### 2.1 Input definition

The first block of the XML-scheme defines the time domain of the input data to be read. The following XML-snippet illustrates a typical setting.

```

<stepValueDefinition>
  <startStop>
    <startStep value="0"/>
    <numSteps value="10"/>
    <startTime value="1e-05"/>
    <delta value="1e-05"/>
    <deleteOffset value="no"/>
  </startStop>
</stepValueDefinition>

```

```
</startStep>
</stepValueDefinition>
```

- delta: time step size in seconds for data import ("CFS time step". Thereby, the time step size can be a whole multiple of the time step provided by the input file to read every 2nd, 3rd etc. time step. If for example the input data time step is 1s and the defined "CFS time step" is 2s, every second time step is read.
- startStep: time offset in multiples of the "CFS time step".
- numSteps: number of time steps to be read.
- startTime: offset in seconds according to the input data time values.
- deleteOffset: delete the offset resulting from startTime. If set to yes and startStep to zero, the first time value of the output data will be the "CFS time step" size.

The first time step which is read from the input file is the time step corresponding to the time `*startStep* *delta* + *startTime*` in seconds. Thereby, the offset resulting from `*startTime*` can be deleted for the output by enabling the `*deleteOffset*`-tag. If data is processed in frequency domain, the same tags are used (`*startTime*` defines the start frequency in this case).

Subsequently, the mesh-based input data is provided by

```
<meshInput id="input">
  <inputFile>
    <hdf5 fileName="pathToInputFile/InpuFile.hdf5"/>
  </inputFile>
</meshInput>
```

in case of using the hdf5 format (e.g. `*openCFS*` simulation file).

`*Enight*` data is considered in the XML-scheme by

```
<meshInput id="input" gridType="fullGrid">
  <inputFile>
    <ensight fileName="pathToInputFile/InputFile.case" fixFVPyramids="yes" readFVMesh="no">
      <variableList>
        <variable CFSVarName="cfsQuantity1" EnightVarName="EnightQuantity1"/>
        <variable CFSVarName="cfsQuantity2" EnightVarName="EnightQuantity2"/>
      </variableList>
    </ensight>
  </inputFile>
</meshInput>
```

where in `*fileName*` the location of the `*Enight*` master file (.case or .encas) needs to be provided and the therein defined quantities (e.g. velocity, pressure) need to be defined by `*EnightVarName*`. In contrast, the quantities of `*hdf5*` files are identified automatically by `*openCFS*`.

## 2.2 Output definition

The processed field data (`*resultQuantity1*` and `*resultQuantity2*`) in the following XML-snippet) is exported in the native hdf5-format. Thereby, the filename is defined in the XML scheme and the default file extension CFS can be adapted, if required. Furthermore, the default compression level of the hdf5-file of 1 can be modified. Furthermore, external files can be enabled, where the field data of each time/frequency step is written to a separate HDF file and the master file includes the mesh data, further file information, and the links to the external files of each time step. To explore hdf5 files and get an understanding of the structure, `*HDFview*` is recommended. The results of multiple filters (e.g., `*filterID1*`, `*filterID2*` in the following example XML) can be either written to all regions or to specified regions of the output mesh as indicated in the snippet.

```
<meshOutput id="OutputFileName" inputFilterIds="filterID1,filterID2">
  <outputFile>
    <hdf5 extension="cfs" compressionLevel="1" externalFiles="no"/>
  </outputFile>
  <saveResults>
    <result resultName="resultQuantity1">
      <allRegions/>
    </result>
  </saveResults>
</meshOutput>
```

```

    </result>
    <result resultName="resultQuantity2">
      <regionList>
        <region name="region1"/>
        <region name="region2"/>
      </regionList>
    </result>
  </saveResults>
</meshOutput>

```

It is important if the exported data will be the input of a subsequent \*openCFS\* simulation, \*openCFS\* variable names must be used for the declaration of field quantities. Thus, for the acoustic PDE, one of the following names must be chosen.

General acoustic and fluid mechanic quantities:

- acouPressure
- acouVelocity
- acouPotential
- acoutIntensity
- fluidMechVelocity
- meanFluidMechVelocity
- fluidMechPressure
- fluidMechDensity
- fluidMechVorticity
- fluidMechGradPressure

Aeroacoustic Source Terms:

- acouRhsLoad (general)
- acouRhsLoadP (PCWE)
- vortexRhsLoad (Vortex Sound Theorie)
- acouDivLighthillTensor (Lighthill's acoustic analogy)

### 3 Aeroacoustic source terms

#### 3.1 Lamb Vector

The Lamb Vector filter computes the Lamb vector  $L$  based on the velocity  $\mathbf{u}$ , vorticity  $\boldsymbol{\omega}$  and the density  $\rho$ .

$$\mathbf{L} = \boldsymbol{\omega} \times \mathbf{u}, \quad (1)$$

with vorticity as

$$\boldsymbol{\omega} = \nabla \times \mathbf{u}. \quad (2)$$

However, it is possible to compute the Lamb vector only based on the velocity, or on the velocity and the vorticity. If only the velocity is defined, the vorticity is computed internally.

- The epsilonScaling Parameter scales the radial basis functions used for computing spatial derivatives [21]. It controls the "smoothness" of the basis function. The smoother the gauss-like surface is, the better the results will be, BUT only until a certain number, when the matrix becomes too ill-conditioned, which will result in very bad results. Typical values: 1e-1 - 1e-4.
- The kScaling parameter is an optional parameter and defines a constant term that is added to the radial basic function.

- The betaScaling parameter defines the slope of a linear term that is added to the radial basis function.
- The logEps Parameter enables a detailed console output (minimal distance, maximal distance, optimized parameters). Therefore, it should only be used if the spatial derivatives are investigated, because it totally spams the console

```
<aeroacoustic type="AeroacousticSource_LambVector" inputFilterIds="..." id="...">
  <RBF_Settings epsilonScaling="1e-4" kScaling="" betaScaling="" logEps=false/>
  <targetMesh>
    <hdf5 fileName=..."/>
  </targetMesh>
  <ResultList>
    <velocity resultName=..."/>
    <vorticity/>
    <density />
    <outputQuantity resultName=..."/>
  </ResultList>
  <regions>
    <sourceRegions>
      <region name=..."/>
    </sourceRegions>
    <targetRegions>
      <region name=..."/>
    </targetRegions>
  </regions>
</aeroacoustic>
```

### 3.2 Lighthill Source Term

The Lighthill source term filter computes aeroacoustic source terms based on Lighthill's analogy for incompressible flows. Therefore, first the Lighthill source term vector is computed

$$\nabla \cdot \mathbf{T} = \nabla \cdot \left( \frac{1}{2} \mathbf{u} \cdot \mathbf{u} \right) + \mathbf{L}, \quad (3)$$

with  $\mathbf{u}$  as velocity, and  $\mathbf{L}$  as Lamb vector, and  $\mathbf{T}$  as the Lighthill stress tensor. Finally, as actual source term, the divergence of the source term vector is computed and established as outputQuantity.

$$\nabla \cdot \nabla \cdot \mathbf{T} = \nabla \cdot \left( \nabla \cdot \left( \frac{1}{2} \mathbf{u} \cdot \mathbf{u} \right) + \mathbf{L} \right) \quad (4)$$

It is possible to compute the Lighthill source term only based on the velocity, or on the velocity and the vorticity. If only the velocity is defined, the vorticity is computed internally and the parameters are the same as for the Lamb vector.

```
<aeroacoustic type="AeroacousticSource_LighthillSourceTerm" inputFilterIds="..." id="...">
  <RBF_Settings epsilonScaling="1e-4" kScaling="" betaScaling="" logEps=false/>
  <sourceSum>true</sourceSum>
  <targetMesh>
    <hdf5 fileName=..."/>
  </targetMesh>
  <ResultList>
    <velocity resultName=..."/>
    <vorticity/>
    <density/>
    <outputQuantity resultName=..."/>
  </ResultList>
  <regions>
    <sourceRegions>
      <region name=..."/>
    </sourceRegions>
    <targetRegions>
      <region name=..."/>
    </targetRegions>
  </regions>
```

```

    </targetRegions>
  </regions>
</aeroacoustic>

```

### 3.3 Lighthill Source Term Vector

The Lighthill source term vector computes a vector corresponding with the  $\nabla \cdot \mathbf{T}$ , where  $\mathbf{T}$  denotes the Lighthill stress tensor, for incompressible flows.

It is possible to compute the Lighthill source term vector only based on the velocity, or on the velocity and the vorticity. If only the velocity is defined, the vorticity is computed internally and the parameters are the same as for the Lamb vector.

```

<aeroacoustic type="AeroacousticSource_LighthillSourceTermVector" inputFilterIds="..." id="...">
  <RBF_Settings epsilonScaling="1e-4" kScaling="" betaScaling="" logEps=false/>
  <sourceSum>true</sourceSum>
  <targetMesh>
    <hdf5 fileName="..."/>
  </targetMesh>
  <ResultList>
    <velocity resultName="..."/>
    <vorticity/>
    <density/>
    <outputQuantity resultName="..."/>
  </ResultList>
  <regions>
    <sourceRegions>
      <region name="..."/>
    </sourceRegions>
    <targetRegions>
      <region name="..."/>
    </targetRegions>
  </regions>
</aeroacoustic>

```

### 3.4 Time Derivative (Simplified PCWE Source Term)

For low flow velocities, convective effects may be neglected for the PCWE, and the resulting source term simplifies to just the time derivative of the incompressible pressure  $\partial p^{ic}/\partial t$ . This is the reason the time derivative filter is placed in the section \*Aeroacoustic Source Terms\*. Of course, the filter can be applied to a different quantity, of which a time derivative is required, as well.

The time derivative of the desired quantity  $\dot{q}(t)$  is computed by a smooth noise-robust differentiator, which suppresses high frequencies and is precise on low frequencies, according to this website. For an efficient and robust calculation the order of the differentiator is set to  $N = 5$  and the time derivative is calculated by

$$\dot{q}(t) = \frac{2(q_1 - q_{-1}) + q_2 - q_{-2}}{8\Delta t}, \quad (5)$$

where the index of  $q$  defines the time step relative to the time step of which the derivative is calculated and  $\Delta t$  is the time step size. The computation only requires the definition of the input quantity (\*inputQuantity\*-tag) and the desired name of the output quantity (\*outputQuantity\*-tag) as indicated below.

```

<timeDeriv1 id="TimeDerivative" inputFilterIds="input">
  <singleResult>
    <inputQuantity resultName="fluidMechPressure"/>
    <outputQuantity resultName="acouRhsLoadP"/>
  </singleResult>
</timeDeriv1>

```

## 4 Acknowledge

We would like to acknowledge the authors of openCFS.

## References

- [1] R. Engelmann, C. Gabriel, S. Schoder, and M. Kaltenbacher. A generic testbody for low-frequency aeroacoustic buffeting. Technical report, SAE Technical Paper, 2020.
- [2] S. Falk, S. Kniesburges, S. Schoder, B. Jakubaß, P. Maurerlehner, M. Echternach, M. Kaltenbacher, and M. Döllinger. 3d-fv-fe aeroacoustic larynx model for investigation of functional based voice disorders. *Frontiers in physiology*, 12:616985, 2021.
- [3] C. Freidhager, P. Maurerlehner, K. Roppert, A. Wurzinger, A. Hauser, M. Heinisch, S. Schoder, and M. Kaltenbacher. Simulationen von strömungsakustik in rotierenden bauteilen zur entwicklung von antriebskonzepten der autos der zukunft. *e & i Elektrotechnik und Informationstechnik*, 138(3):212–218, 2021.
- [4] C. Freidhager, S. Schoder, and M. Kaltenbacher. The influences of spatial and temporal discretization in flow simulation on lighthill’s aeroacoustic source terms applied to a turbocharger. In *AIAA AVIATION 2020 FORUM*, page 2546, 2020.
- [5] C. Freidhager, S. Schoder, P. Maurerlehner, A. Renz, S. Becker, and M. Kaltenbacher. Applicability of two hybrid sound prediction methods for assessing in-duct sound absorbers of turbocharger compressors. *Acta Acustica*, 6:37, 2022.
- [6] M. Kaltenbacher. *Computational Acoustics*. CISM International Centre for Mechanical Sciences. Springer International Publishing, 2017.
- [7] M. Kaltenbacher, M. Escobar, I. Ali, and S. Becker. Numerical Simulation of Flow-Induced Noise Using LES/SAS and Lighthill’s Acoustics Analogy. *International Journal for Numerical Methods in Fluids*, 63(9):1103–1122, 2010.
- [8] M. Kaltenbacher and S. Floss. Nonconforming finite elements based on nitsche-type mortaring for inhomogeneous wave equation. *Journal of theoretical and computational acoustics*, 26(03):1850028, 2018.
- [9] M. Kaltenbacher, C. Freidhager, and S. Schoder. Modelling and numerical simulation of the noise generated by automotive turbocharger compressor. Technical report, SAE Technical Paper, 2020.
- [10] M. Kaltenbacher, A. Hüppe, J. Grabinger, and B. Wohlmuth. Modeling and Finite Element Formulation for Acoustic Problems Including Rotating Domains. *AIAA Journal*, 2016.
- [11] M. Kaltenbacher and S. Schoder. Physical models for flow: Acoustic interaction. In *Waves in Flows*, pages 265–353. Springer, 2021.
- [12] F. Kraxberger, A. Wurzinger, and S. Schoder. Machine-learning applied to classify flow-induced sound parameters from simulated human voice. *arXiv preprint arXiv:2207.09265*, 2022.
- [13] M. Lasota, P. Šidlof, M. Kaltenbacher, and S. Schoder. Impact of the sub-grid scale turbulence model in aeroacoustic simulation of human voice. *Applied Sciences*, 11(4):1970, 2021.
- [14] M. Lasota, P. Šidlof, P. Maurerlehner, M. Kaltenbacher, and S. Schoder. Anisotropic minimum dissipation subgrid-scale model in hybrid aeroacoustic simulations of human phonation. *arXiv preprint arXiv:2301.00606*, 2023.
- [15] P. Maurerlehner, S. Schoder, C. Freidhager, A. Wurzinger, A. Hauser, F. Kraxberger, S. Falk, S. Kniesburges, M. Echternach, M. Döllinger, et al. Efficient numerical simulation of the human voice. *e & i Elektrotechnik und Informationstechnik*, 138(3):219–228, 2021.
- [16] P. Maurerlehner, S. Schoder, J. Tieber, C. Freidhager, H. Steiner, G. Brenn, K.-H. Schäfer, A. Ennemoser, and M. Kaltenbacher. Aeroacoustic formulations for confined flows based on incompressible flow data. *Acta Acustica*, 6:45, 2022.
- [17] S. Schoder. cpcwe–perturbed convective wave equation based on compressible flows. *arXiv preprint arXiv:2209.11410*, 2022.
- [18] S. Schoder. Pcwe for fsai–derivation of scalar wave equations for fluid-structure-acoustics interaction of low mach number flows. *arXiv preprint arXiv:2211.07490*, 2022.
- [19] S. Schoder and F. Czwiolong. Dataset fan-01: Revisiting the eaa benchmark for a low-pressure axial fan. *arXiv preprint arXiv:2211.12014*, 2022.
- [20] S. Schoder, C. Junger, and M. Kaltenbacher. Computational aeroacoustics of the eaa benchmark case of an axial fan. *Acta Acustica*, 4(5):22, 2020.
- [21] S. Schoder, C. Junger, K. Roppert, and M. Kaltenbacher. Radial basis function interpolation for computational aeroacoustics. In *AIAA AVIATION 2020 FORUM*, page 2511, 2020.

- [22] S. Schoder, C. Junger, M. Weitz, and M. Kaltenbacher. Conservative source term interpolation for hybrid aeroacoustic computations. In *25th AIAA/CEAS aeroacoustics conference*, page 2538, 2019.
- [23] S. Schoder and M. Kaltenbacher. Hybrid aeroacoustic computations: State of art and new achievements. *Journal of Theoretical and Computational Acoustics*, 27(04):1950020, 2019.
- [24] S. Schoder, M. Kaltenbacher, and K. Roppert. Helmholtz’s decomposition applied to aeroacoustics. In *25th AIAA/CEAS Aeroacoustics Conference*, 2019-2561.
- [25] S. Schoder, M. Kaltenbacher, É. Spieser, H. Vincent, C. Bogey, and C. Bailly. Aeroacoustic wave equation based on pierce’s operator applied to the sound generated by a mixing layer. In *28th AIAA/CEAS Aeroacoustics 2022 Conference*, page 2896, 2022.
- [26] S. Schoder, F. Kraxberger, S. Falk, A. Wurzinger, K. Roppert, S. Kniesburges, M. Döllinger, and M. Kaltenbacher. Error detection and filtering of incompressible flow simulations for aeroacoustic predictions of human voice. *The Journal of the Acoustical Society of America*, 152(3):1425–1436, 2022.
- [27] S. Schoder, I. Lazarov, and M. Kaltenbacher. Numerical investigation of a deep cavity with an overhanging lip considering aeroacoustic feedback mechanism. *arXiv preprint arXiv:2006.03279*, 2020.
- [28] S. Schoder, P. Maurerlehner, A. Wurzinger, A. Hauser, S. Falk, S. Kniesburges, M. Döllinger, and M. Kaltenbacher. Aeroacoustic sound source characterization of the human voice production-perturbed convective wave equation. *Applied Sciences*, 11(6):2614, 2021.
- [29] S. Schoder, E. Museljic, F. Kraxberger, and A. Wurzinger. Post-processing subsonic flows using physics-informed neural networks. In *2023 AIAA AVIATION Forum*, 2022.
- [30] S. Schoder and K. Roppert. Learning expertise actively to model domain knowledge (lead) with application to human phonation. *arXiv*, 2022.
- [31] S. Schoder and K. Roppert. opencfs: Open source finite element software for coupled field simulation–part acoustics. *arXiv preprint arXiv:2207.04443*, 2022.
- [32] S. Schoder, K. Roppert, and M. Kaltenbacher. Helmholtz’s decomposition for compressible flows and its application to computational aeroacoustics. *SN Partial Differ. Equ. Appl.*, pages 1–20, 2020.
- [33] S. Schoder, K. Roppert, and M. Kaltenbacher. Postprocessing of direct aeroacoustic simulations using helmholtz decomposition. *AIAA Journal*, pages 1–9, 2020.
- [34] S. Schoder, K. Roppert, M. Weitz, C. Junger, and M. Kaltenbacher. Aeroacoustic source term computation based on radial basis functions. *International Journal for Numerical Methods in Engineering*, 121(9):2051–2067, 2020.
- [35] S. Schoder, J. Schmidt, A. Furlinger, and M. Kaltenbacher. Quantification of the acoustic emissions of an electric ducted fan unit. In *2022 Delft International Conference on Urban Air-Mobility: DICUAM 2022*, 2022.
- [36] S. Schoder, M. Weitz, P. Maurerlehner, A. Hauser, S. Falk, S. Kniesburges, M. Döllinger, and M. Kaltenbacher. Hybrid aeroacoustic approach for the efficient numerical simulation of human phonation. *The Journal of the Acoustical Society of America*, 147(2):1179–1194, 2020.
- [37] S. Schoder, A. Wurzinger, C. Junger, M. Weitz, C. Freidhager, K. Roppert, and M. Kaltenbacher. Application limits of conservative source interpolation methods using a low mach number hybrid aeroacoustic workflow. *Journal of Theoretical and Computational Acoustics*, 29(01):2050032, 2021.
- [38] S. J. Schoder. *Aeroacoustic analogies based on compressible flow data*. PhD thesis, Wien, 2018.
- [39] S. J. Schoder, C. Junger, M. Weitz, and M. Kaltenbacher. Conservative interpolation of aeroacoustic sources in a hybrid workflow applied to fan. *arXiv preprint arXiv:2009.02341*, 2020.
- [40] M. Tautz, K. Besserer, S. Becker, and M. Kaltenbacher. Source formulations and boundary treatments for lighthill’s analogy applied to incompressible flows. *AIAA Journal*, 56(7):2769–2781, 2018.
- [41] L. Tieghi, S. Becker, A. Corsini, G. Delibra, S. Schoder, and F. Czwielong. Machine-learning clustering methods applied to detection of noise sources in low-speed axial fan. In *2022 Turbomachinery Technical Conference & Exposition: ASME Turbo Expo 2022*, 2022.
- [42] L. Tieghi, S. Becker, A. Corsini, G. Delibra, S. Schoder, and F. Czwielong. Machine-learning clustering methods applied to detection of noise sources in low-speed axial fan. *Journal of Engineering for Gas Turbines and Power*, 145(3):031020, 2023.
- [43] J. Valášek, M. Kaltenbacher, and P. Sváček. On the application of acoustic analogies in the numerical simulation of human phonation process. *Flow, Turbulence and Combustion*, 102(1):129–143, 2019.
- [44] M. Weitz, S. Schoder, and M. Kaltenbacher. Numerical investigation of the resonance behavior of flow-excited helmholtz resonators. *PAMM*, 19(1):e201900033, 2019.

- [45] S. Zörner, P. Šidlof, A. Hüppe, and M. Kaltenbacher. Flow and acoustic effects in the larynx for varying geometries. *Acta Acustica united with Acustica*, 102(2):257–267, 2016.